Electronic Supplementary Information

Near-Infrared Light Activated Photosensitizer with Specific Imaging of Lipid Droplets Enables Two-Photon Excited Photodynamic Therapy

Tengdie Wu, Xin Lu, Zhipeng Yu, Xiaojiao Zhu, Jie Zhang, Lianke Wang,* Hongping Zhou*

Institutes of Physical Science and Information Technology, College of Chemistry and Chemical Engineering, Anhui University, Anhui Province Key Laboratory of Chemistry for Inorganic/Organic Hybrid Functionalized Materials, Key Laboratory of Structure and Functional Regulation of Hybrid Materials (Anhui University), Ministry of Education, Hefei, 230601, People's Republic of China

E-mail address: wanglianke2009@163.com, zhpzhp@263.net

TABLE OF CONTENT

1 Experimental and Methods

1.1 Materials

Chemicals for synthesis and fluorescence detection were purchased from commercial sources (Aladdin, Macklin, Sigma-Aldrich, Bioquest and Thermo), and used directly without further purification, including 9,10-anthracenediylbis (methylene) - dimalonic acid (ABDA), Singlet Oxygen Sensor Green (SOSG), BODIPY 493/503, 2,2,6,6-Tetramethylpiperidine(TEMP), 5,5-Dimethyl-1-pyrroline N-oxide (DMPO), 2,7-dichlorodihydrofluorescein diacetate (DCFH-DA), Calcein – AM / PI Double Stain Kit and apoptosis/ necrosis kit (Annexin V-FITC/PI), dulbecco's modified eagle medium (DMEM). Human cervical cancer cell (HeLa cells) and human hepatocellular carcinoma cell (HepG2) were purchased from BeNa culture collection. All female ICR mice were given by the Laboratory Animal Center of the Shanxi Medical University. All the animal experiments were performed in compliance with the relevant laws and institutional guidelines and approved by the Animal Experiments and Care regulations of Anhui University.

1.2 General instruments

^{1}H and ^{13}C-NMR spectra were recorded on a Bruker Avance spectrometer using d- chloroform as solvent (400 MHz for ^{1}H NMR and 100 MHz for ^{13}C NMR) and tetramethylsilane (TMS) as internal standard. Mass spectra were performed on a Thermo Fisher Scientific LTQ Orbitrap mass spectrometer equipped with an electrospray ion source (ESI). UV-vis absorption and fluorescence spectra were recorded on a UV-265 spectrophotometer and a Hitachi F-7000 fluorescence spectrophotometer, respectively. Two-photon emission fluorescence (TPEF) spectra were measured with femtosecond laser pulse and Ti: sapphire system (adjustable output wavelength: 680-1080 nm, 80 MHz, 140 fs) as the light source. Two-photon excitation fluorescence cross section was analyzed by two-photon excitation fluorescence method using rhodamine B (Rh B) as references. Fluorescence quantum yields were determined by FLUORMAX-4P spectrophotometer. Fluorescent lifetime was carried out on a FLUOROMAX PLUS. Nano X-band system from Bruker (Germany) was used to record the electron paramagnetic resonance (EPR) spectra to assess $^{1}O_2$ production by the irradiated sample. Room-temperature EPR measurement was performed at School of Chemistry and Chemical Engineering, Anhui University. Single-crystal X-ray crystallographic data were collected on a Bruker Smart APEX II diffractometer with a CCD area detector. Confocal fluorescence imaging was performed on ZEISS710 and Olympus FV 1200 MPE-share confocal laser scanning microscope (CLSM). Small animals' fluorescence imaging was captured by the LB983 NC100 living imaging system (Berthold co. Ltd.).

1.3 The measurement of two-photon absorption cross section

Two-photon-absorption (TPA) cross section was determined by using a femto-second (fs) fluorescence measurement technique as described. The standard sample is Rhodamine B (Rh B) with a concentration of 1.0 mM. The concentration of **6DBF$_2$** was 1.0 mM.

TPA cross section (δ) can be calculated using the following formula:

$$\delta=\delta_r \frac{\Phi r c r n r F s}{\Phi s c s n s F r}$$

where the subscripts s and r stand for the sample and reference molecules, respectively.

δ is the two-photon absorption cross section, c, n, and Φ are the concentration, refractive index, and fluorescence quantum yield, F is two-photon fluorescence integral area.

1.4 Measurements of $^1O_2$ and $\cdot O_2^-$ Generation by Electron Paramagnetic Resonance (EPR)

The EPR assay was carried out with a Bruker Nano x-band spectrometer using 5,5-dim ethyl-1-pyrroline N-oxide (DMPO) and 2,2,6,6-tetramethylpiperidine (TEMP) as spin-trap agent. **6DBF$_2$** was dissolved in DMSO at a dilution of 1 mM, take 100 μL **6DBF$_2$** soluti on each time and then 10 μL TEMP or DMPO was added into solution without and wi th irradiation (LED laser: 40 mW/cm^2 and femto-second laser irradiation (820 nm,100 mW), for 5 minutes respectively. Finally, the EPR signal was recorded at room temper ature.(Typical experimental conditions: frequency= 9.638850 GHz, power= 6.310 mW, m odulation frequency= 100.00 kHz, modulation amplitude= 1G, and time constant=1.28 m s)

1.5 UV-vis spectra of 6DBF$_2$ in H_2O at different concentration

Stocking solution of **6DBF$_2$** (1 mM) were prepared in DMSO, 3 μL or 30 μL of **6DBF$_2$** was added into 3 mL of water every time, and the solution was placed in a quartz cell with an optical path length of 1 cm, and the UV-Vis spectra were recorded at room temperature.

1.6 photostability test in vitro

The photostability of **6DBF$_2$** was investigated in H_2O, solution of **6DBF$_2$**(10 μM) in 1 cm quartz cell was irradiated by using white light (20 mW/cm^2) or two-photon laser (820 nm, 100 mW/cm^2) for 60 min. The absorbance of the **6DBF$_2$** solution was recorded every 10 min.

1.7 Singlet dioxygen ($^1O_2$) generation detection

The quantum yield of $^1O_2$ was determined with ABDA as $^1O_2$-trapping agent and Rose Bengal (RB) as the standard. Briefly, 2 mL of water solution was mixed with 20 uL **6DBF$_2$** (1 mM) or RB (1 mM) and 20 uL ABDA (7.5 mM). Then the cuvette was exposed to LED light (400-700 nm, 20 mW/cm^2) irradiation for different time.

The $^1O_2$ quantum yield of the 6DBF$_2$ was calculated using the following formula:

$$\Phi = \Phi_{RB} \frac{K * A_{RB}}{K_{RB} * A}$$

where K and K_{RB} are the decomposition rate constants of ABDA in the presence of 6DBF$_2$ and RB, respectively. A and A_{RB} represent the light absorbance of the **6DBF$_2$** and RB, respectively, which are determined by integration of the absorption bands ranged in 400–700 nm, Φ_{RB} is the $^1O_2$ quantum yield of RB with 0.75 in water.

1.8 In vitro ROS detection

2, 7-dichlorodifluorescein diacetate (DCFH-DA) was used as the ROS indicator. Stocking solution of DCFH-DA (2.0 mM, under dark) and NaOH (0.01 M) were firstly prepared in HPLC grade DMSO and distilled water, respectively. DCFH-DA solution (100 μL, 2 mM) was activated by NaOH aqueous solution (0.8 mL, 0.01 M) for 30 min in dark at room temperature, then 4.1 mL of PBS buffer solution was added in the activated solution. Finally, stocking solution of **6DBF$_2$**(50 μL, 1 mM) was added into it. Fluorescence spectra were collected before and after exposure to white LED lamp (400−700 nm, 20 mW/cm^2) with different time (0, 30, 60, 90, 120, 150, 180, 210, 240 s). The fluorescence intensity at 525 nm was recorded to indicate the ROS generation.

1.9 In vitro $^1O_2$ detection

The generation of $^1O_2$ was detected using 9,10-anthracenediyl-bis-(methylene)-dimalonic acid (ABDA) as the $^1O_2$-monitoring agent. The DMSO solution of ABDA (7.5 mM, 20 μL) were added into 2 mL dyes (10 μM) in dark condition. Then the cuvette was exposed to white LED lamp (400−700 nm, 20 mW/cm^2) irradiated for various time (0 - 360 s). The decrease of the absorption of ABDA at 378 nm was obtained at different amounts of irradiation time to detect the decay rate of the photosensitizing process.

1.10 Cell Culture and Image

All cell lines were incubated in DMEM containing 10% of FBS and antibiotics (100 units per mL penicillin and 100 μg/mL streptomycin) at 37 °C in a humidified atmosphere containing 5% of CO_2. In fluorescence imaging experiments, the cells were planted into glass bottom dishes (15 × 15 mm) at density of 10^4 for confocal, co-location experiments and at density of 10^6 for live/dead experiment (AM/PI). After 6DBF$_2$ was added and cultivated for 30 min at 37 °C, the dishes were washed with PBS (pH = 7.2) for three times. The cell images were acquired via ZEISS710 and Olympus FV 1200 MPE-share confocal laser scanning microscope with 10× or 60 × objective lens.

1.11 AM/PI Staining

Living cells were stained with green fluorescence by calcein acetoxymethyl ester (calcein AM), and dead cells were stained with red fluorescence by propidium iodide (PI). HepG2 cells were planted onto confocal dishes and incubated for 48 h. Then the cells were further treated with 400 uL dye diluent and 5 Ul of Calcein-AM stain after 6DBF$_2$ (0.5 μM)was added for 30 min. Co-incubated for 20 min, the cell confocal image was observed at different light irradiation time period using CLSM. (Calcein-AM: λ_{ex}: 488 nm, λ_{em}: 510 - 540 nm, PI: λ_{ex}: 561 nm, λ_{em}: 590 - 620 nm)

1.12 Intracellular $^1O_2$ Imaging

SOSG was used for the intracellular $^1O_2$ indicator. HepG2 cells were seeded in the glass bottom dishes and incubated about 48 h for adhering. And then, HepG2 cells were incubated with **6DBF$_2$** (0.5 μM) for 30 min for cell uptake followed by incubation with SOSG (1 μM) for 30 min. Subsequently, wash the cells with PBS and further exposed to the white light irradiation (0, 3, 6 min) or femtosecond laser irradiation at 820 nm (0, 3, 6 min). The green fluorescence was immediately captured by CLSM. (λ_{ex} : 488 nm; λ_{em} : 500 - 530 nm).

1.13 Subcellular Colocalization Assay

HepG2 cells were seeded into 15mm × 15mm confocal dishes and incubated for 48 h. After incubated with **6DBF$_2$** (0.5 μM) for 30 min, wash the cells with PBS and then stained by 1 μL BODIPY493/503 for 10min. After finishing staining, the cells were washed with PBS for three times. Cells were imaged under confocal microscope.

1.14 Mechanisms of Cell Death using Apoptosis/Necrosis Kit (Annexin V-FITC/PI)

Annexin V-FITC/propidium iodide (PI) staining reagents were used to study the cell death pathway.HepG2 cells were planted onto confocal dishes and grew to suitable density (1×10^4 cells). Then **6DBF$_2$** (0.5 μM) was added to co-culture for 30 min, wash the cells with PBS and subsequently disposed with 400 μL binding buffer and stained by 5 μL Annexin V-FITC and 5 μL PI in a cool and dark atmosphere for 15 min. Finally, the co-stained HepG2 cells were observed by CLSM and traced with 10 min of 820 nm laser irradiation. (Annexin V-FITC: λ_{ex} : 488 nm; λ_{em} : 500-540 nm, PI: λ_{ex} = 561 nm; λ_{em} : 630-670 nm)

1.15 Normal hepatic tissues, HepG2 cancer tissues and fatty liver tissues imaging

The tissue with the thickness of 100 μm, were stained with **6DBF$_2$** (1 mM) at room temperature for 2 h. The tissue sample was washed three times with phosphate-buffered saline (PBS, pH = 7.2) before one-photon and two-photon imaging.

1.16 Cellular uptake mechanism studies

Dish 1: the cells were incubated with **6DBF$_2$** for 30 min at 4 °C. Dish 2: the cells were incubated with **6DBF$_2$** for 30 min at 37 °C. Dish 3: the cells were pretreated with chloroquine inhibitors for 15 min , PBS was then used to wash the cells, and the cells were further treated 0.5 μM of **6DBF$_2$** for 20 min. After finishing staining, the cells were washed with PBS for three times. Cells were imaged under confocal microscope.

1.17 Transportation into lipid droplets mechanism studies

HepG2 cells were planted onto confocal dishes and incubated for 48 h. After adding **6DBF$_2$** into the dish, the cells were captured by confocal microscopy every 10 second.

1.18 In vivo Fluorescence Imaging

6DBF$_2$ (1 mM,100 μL) was injected intratumorally, then mice was anesthetized with 20% isofluorane in oxygen. Afterwards, the whole-body fluorescence images were captured by the LB983 NC100 imaging system (Berthold co. Ltd.) at 0, 0.5, 3, 6, 9 and 12 hours after injections. After the 12 h later, mice were sacrificed and the major organs (heart, liver, spleen, lung, kidney and tumor) were collected. The luminescence in each organ were recorded with an in vivo imaging system (LB983 NC100).

1.19 In vivo Evaluation

Cell's suspension (108 cells/mL, H22 cells) was obtained and then subcutaneously injected at the female ICR mice (28-35 days). Then the H22-bearing mice were kept in SPF condition, protected from light and feed and watered freely. The tumor volume within the mouse was daily monitored. When the tumor volume reached approximately 100mm^3, the animals were

randomly divided into four groups and treated as described below: PBS as control(group I), PBS+ 820 nm fs laser (group II), **6DBF$_2$** (group III), and **6DBF$_2$** +820 nm fs laser (group IV).It is notable that only a single-dose injection was employed during in vivo treatment process.

The tumor volume and body weight of each mouse was recorded every three days for 18 days. According to the volume formula: volume (mm^3) = (length × $width^2$)/2; After treatment, tumors were weighed and dissected, tumor and organ tissues (heart, liver, spleen, lung, kidney) were collected, photographed by H&E staining.

1.20 X-ray Crystallography

Single-crystal diffraction data was measured on a Bruker APEX-II CCD diffractometer by using the graphite monochromated MoKa radiation (λ = 0.71073 Å) at 296 K. SADABS-2014/5 (Bruker, 2014/5) was used for absorption correction. Subsequent steps were run under Olex2: the molecular structure was solved with SHELXT structure solution program using Intrinsic Phasing and refined with the SHELXL refinement package using Least Squares minimization. All non-hydrogen atoms were refined anisotropically. CCDC 2213642 contains the supplementary crystallographic data for this paper. This data can be obtained free of charge via www.ccdc.cam.ac.uk/data_request/cif, or by emailing data_request@ccdc.cam.ac.uk, or by contacting The Cambridge Crystallographic Data Centre, 12 Union Road, Cambridge CB2 1EZ, UK; fax: + 44 1223 336033.

2. Synthesis and Characterization

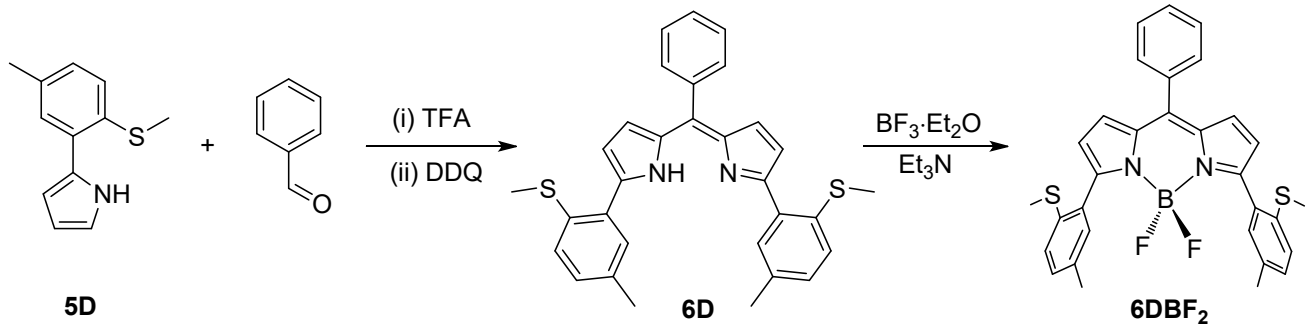

Scheme S1. Synthetic route of **6DBF$_2$**.

Preparation of 6D: 2-(5-methyl-2-(methylthio)phenyl)-1H-pyrrole (**5D**) was prepared according to the reported procedure. [1] The synthesis of ligand **6D** was referred to the reported method.[2, 3] A 100 mL schlenck tube containing a magnetic stirring bar was charged with **5D** (3.5 g, 17.21mmol) and CH_2Cl_2 (30 mL). The solution was degassed for 30 minutes by dinitrogen. After benzaldehyde (0.92 g, 8.6 mmol) and TFA (0.2 mL, 2.58 mmol) was added in this order, the resulting mixture was stirred at room temperature for 4 h. 2,3-Dichloro-5,6-dicyano-p-benzoquinone (DDQ, 1.96 g, 8.6 mmol) was added, and the reaction mixture was further stirred at room temperature for 4.5 h. The resulting suspension was washed with saturated aqueous $NaHCO_3$ (200 mL × 3), and the organic layer was dried via Na_2SO_4 and concentrated under reduced pressure. The resulting residue was purified by column chromatography (silica gel, AcOEt/petroleum ether = 75/1 as an eluent) to give the title product as red solid. Yield: 71%.**^{1}H NMR** (400 MHz, acetone-d_6, ppm) δ 7.6655-7.6626 (d, J = 1.16 Hz, 2H), 7.5844-7.5330 (m, 5H), 7.2968-7.2767 (d, J = 8.12 Hz, 2H), 7.2396-7.2164 (d, J =

9.28 Hz, 2H), 6.9026-6.8917 (d, *J* = 4.36 Hz, 2H), 6.6048-6.5942 (d, *J* = 4.24 Hz, 2H), 2.8056 (s, 1H), 2.3653 (s, 6H), 2.2698 (s, 6H). **^{13}C NMR** (100 MHz, acetone-d_6, ppm) δ 141.90, 138.26, 135.90, 134.93, 131.99, 131.52, 131.30, 130.88, 129.69, 128.91, 128.66, 126.64, 20.72, 15.95.**ESI-FTMS** (in acetone, m/z): calculated for $C_{31}H_{29}N_2S_2$ $[M+H]^+$: 493.169, found: 493.1761.

Preparation of 6DBF$_2$: **6DBF$_2$** was prepared according to the reported procedure.[4, 5] To a solution of ligand **6D** (98.54 mg, 0.2 mmol) in CH_2Cl_2 (2.5 mL) was added Et_3N (0.4 mL, 2.88 mmol) and BF_3•Et_2O (0.4 mL, 2.96 mmol), and further stirred at room temperature. After 2 h, the resulting solution was added ethanol (2.5 mL) and allowed to evaporate slowly. The dark red crystals suitable for X-ray diffraction were obtained by filtration and washed quickly by ethanol after 5 days. Yield: 63%.**^{1}H NMR** (400 MHz, $CDCl_3$, ppm) δ 7.6546-7.6382 (m, 2H), 7.5953-7.5140 (m, 3H), 7.4008 (s, 2H), 7.2237-7.2035 (d, *J* = 8.08 Hz, 2H), 7.1443-7.1239 (d, *J* = 8.16 Hz, 2H), 6.8859-6.8753 (d, *J* = 4.24 Hz, 2H), 6.5769-6.5664 (d, *J* = 4.2 Hz, 2H), 2.3342 (s, 6H), 2.2982 (s, 6H). **^{13}C NMR** (100 MHz, CD_2Cl_2, ppm) δ 156.15, 144.29, 134.55, 134.22, 133.57, 133.36, 131.51, 130.58, 129.96, 129.74, 129.55, 129.03, 127.55, 125.88, 121.15, 19.80, 15.94. **APCI-FTMS** (in CH_3OH, m/z): calculated for $C_{31}H_{27}N_2S_2$ $[M-F]^+$: 521.1687, found: 521.1693.

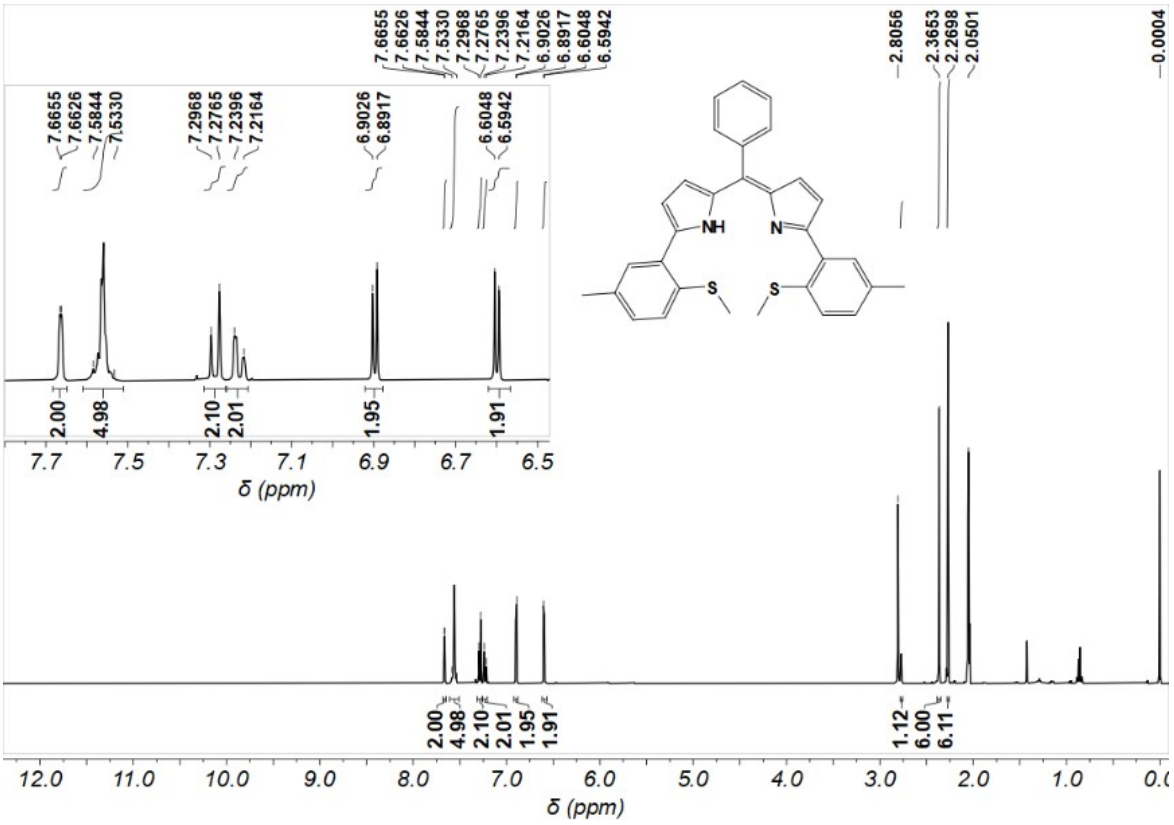

Figure S1. ^{1}H NMR spectrum of **6D** in *d*-acetone.

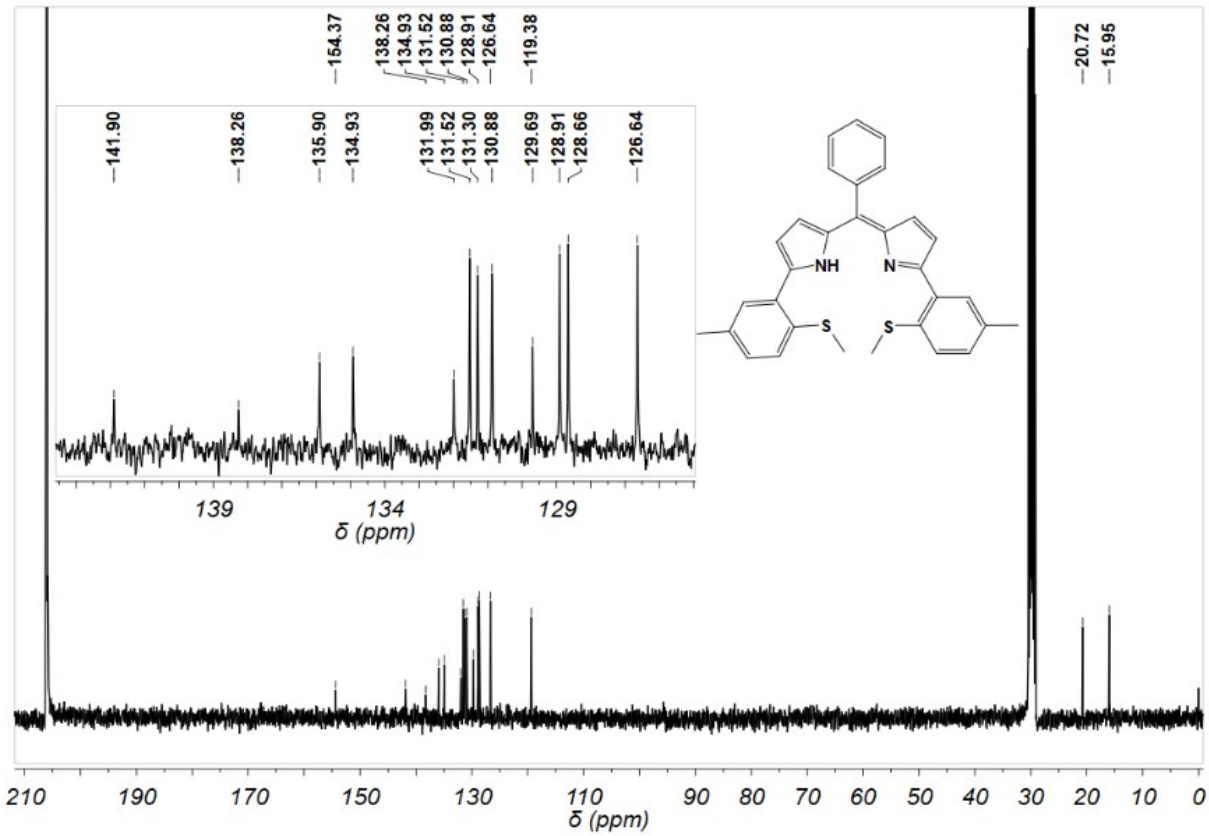

Figure S2. ^{13}C NMR spectrum of **6D** in *d*-acetone.

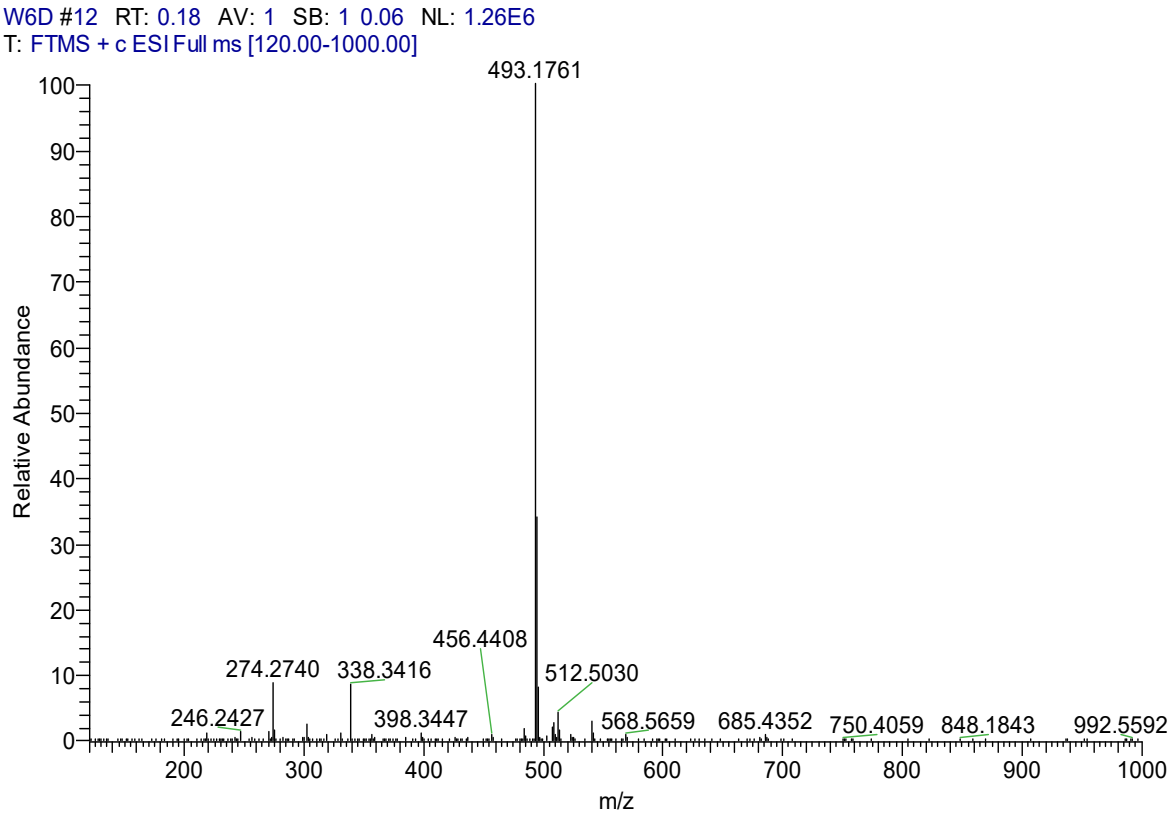

Figure S3. ESI-FTMS of **6D** in acetone.

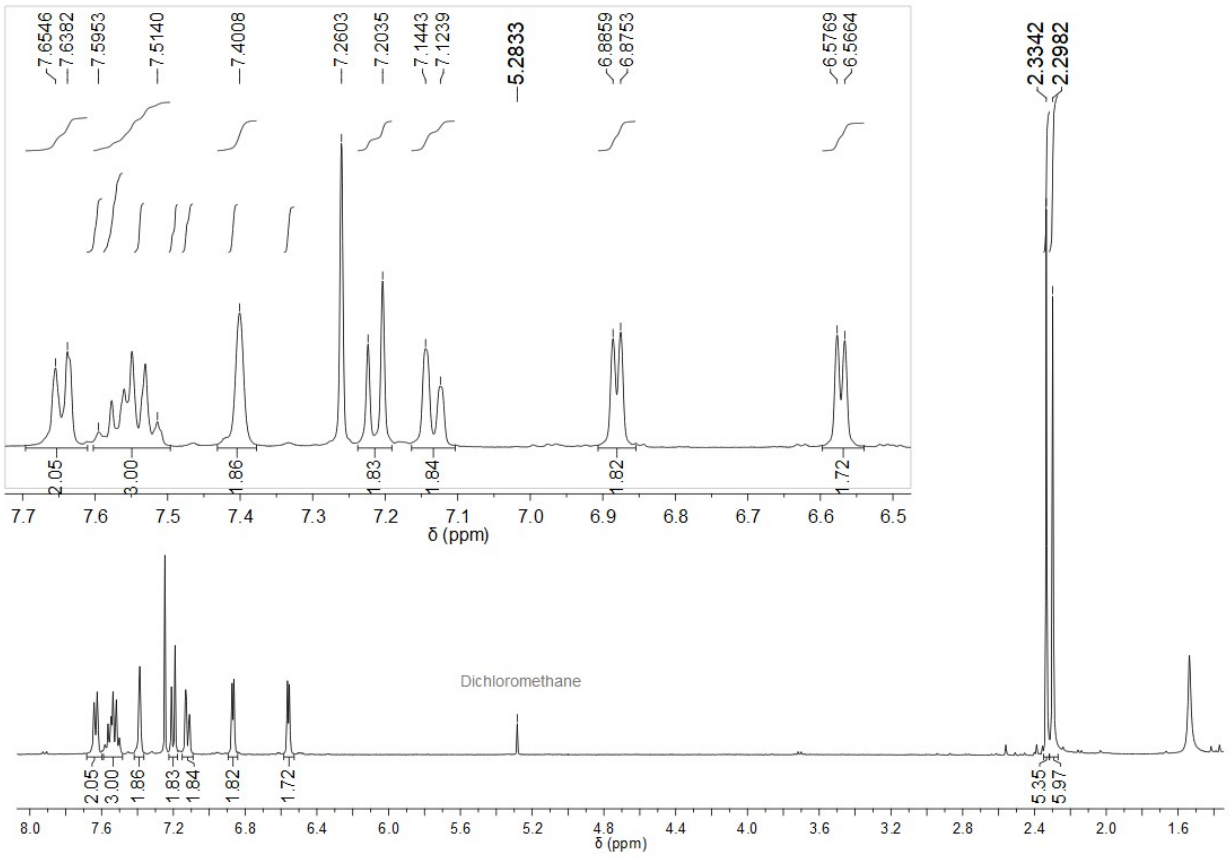

Figure S4. ^{1}H NMR spectrum of **6DBF$_2$** in $CDCl_3$.

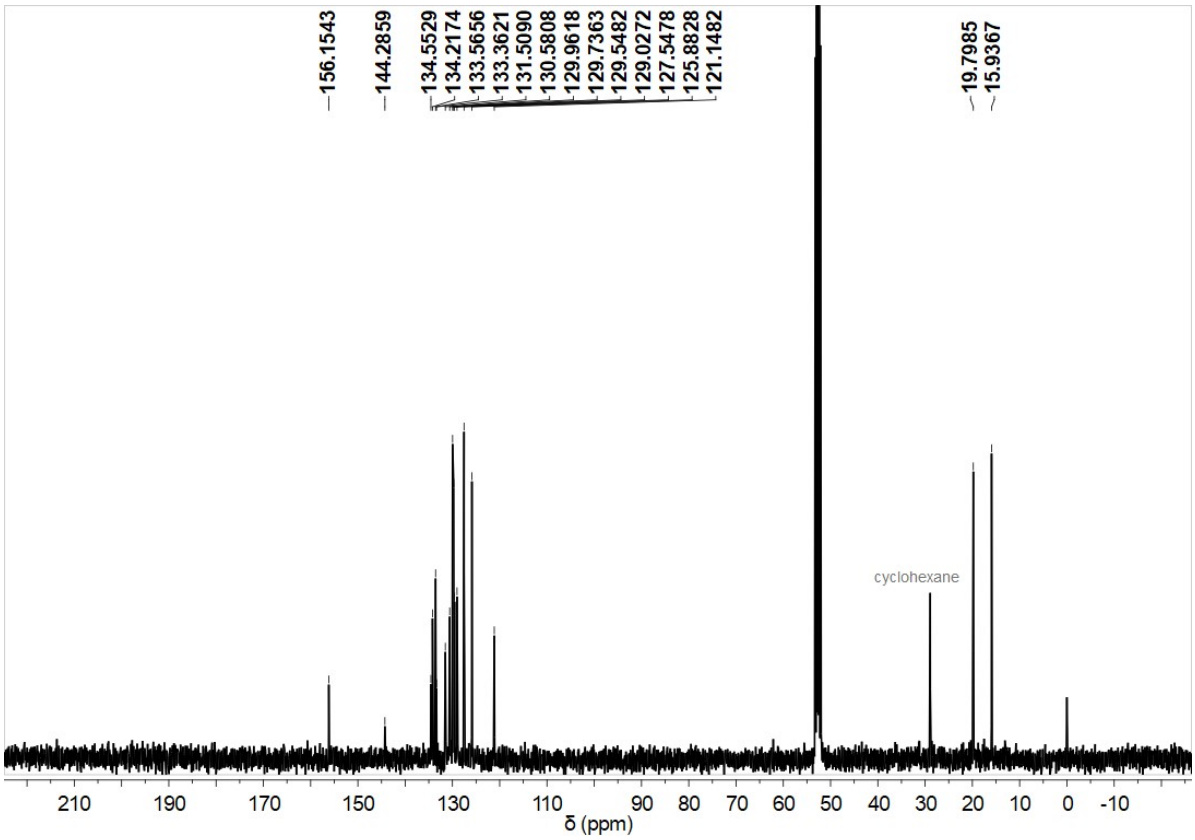

Figure S5. ^{13}C NMR spectrum of **6DBF$_2$** in CD_2Cl_2.

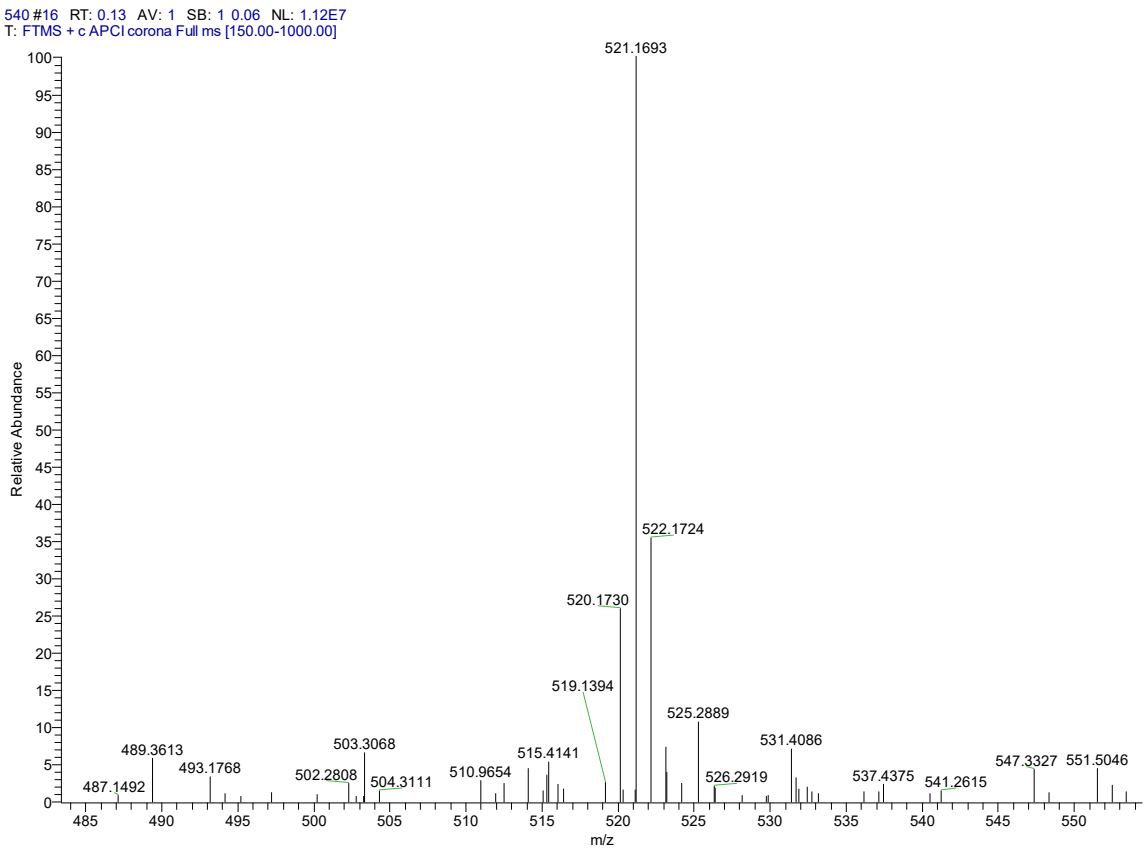

Figure S6. ESI-FTMS of **6DBF$_2$** in methanol.

3. Supplementary Figures

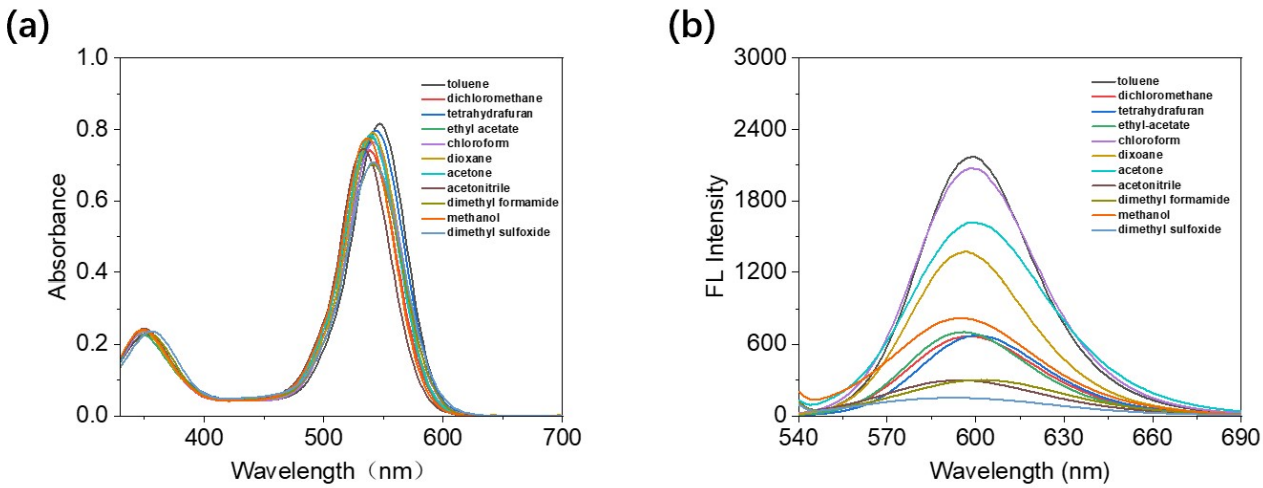

Figure S7. (**a**) UV-vis spectra and (**b**) fluorescence spectra of **6DBF$_2$** (10 μM) in various solvents.

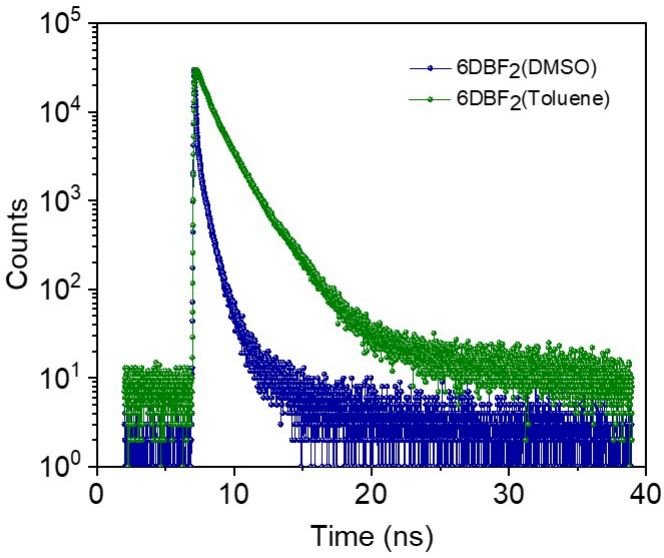

Figure S8. Fluorescence lifetime of **6DBF$_2$** (10 μM) in DMSO and toluene.

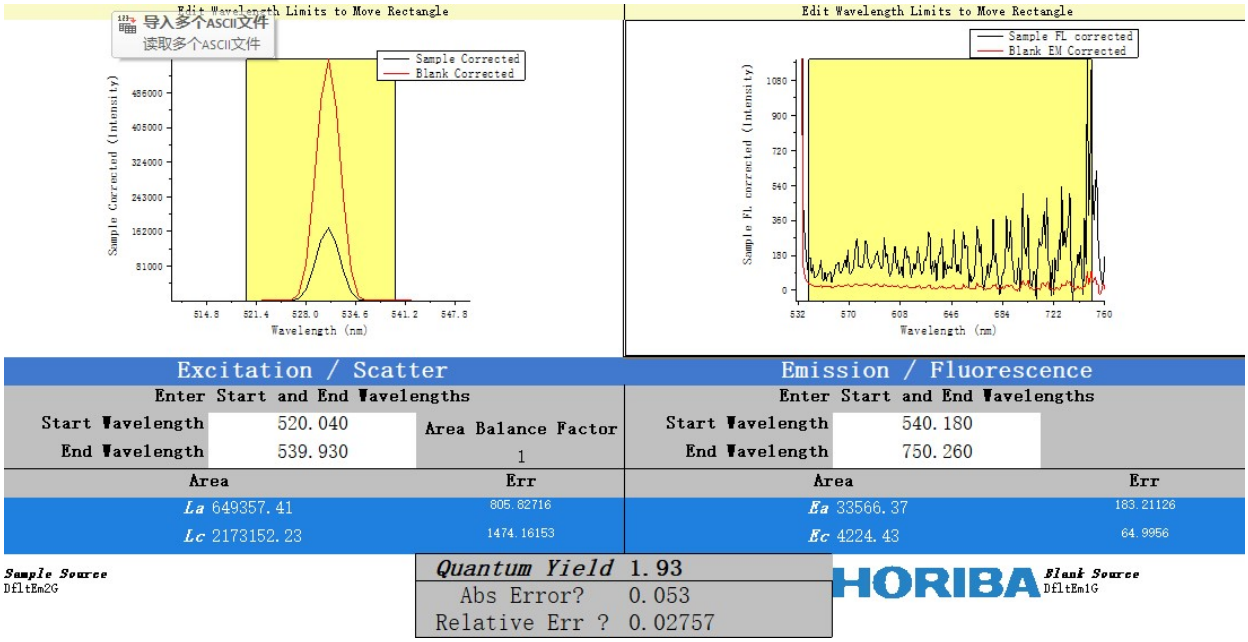

Figure S9. Quantum yield of **6DBF$_2$** in DMSO.

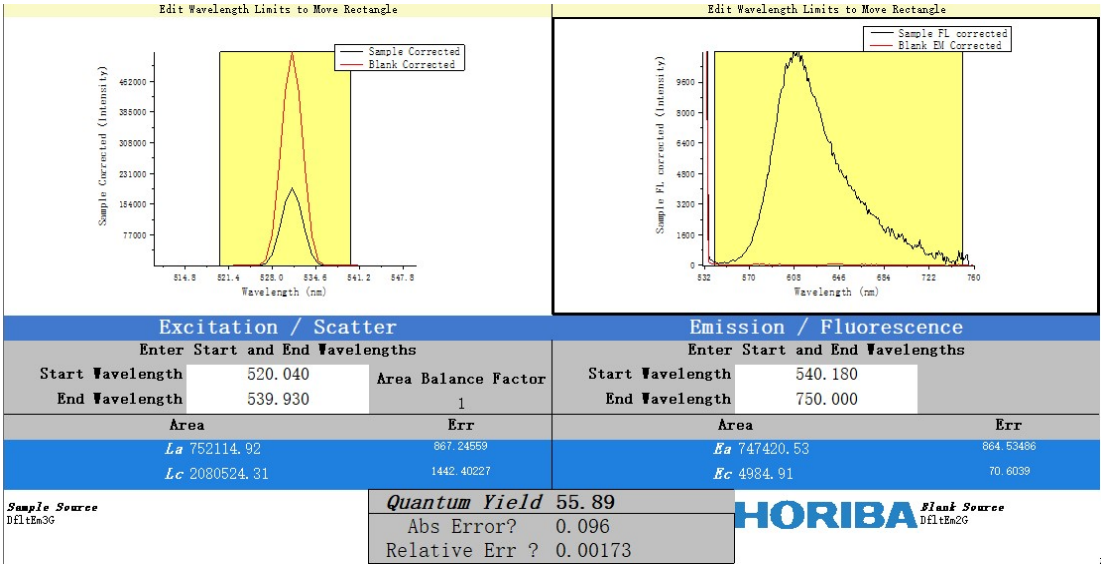

Figure S10. Quantum yield of **6DBF$_2$** in toluene.

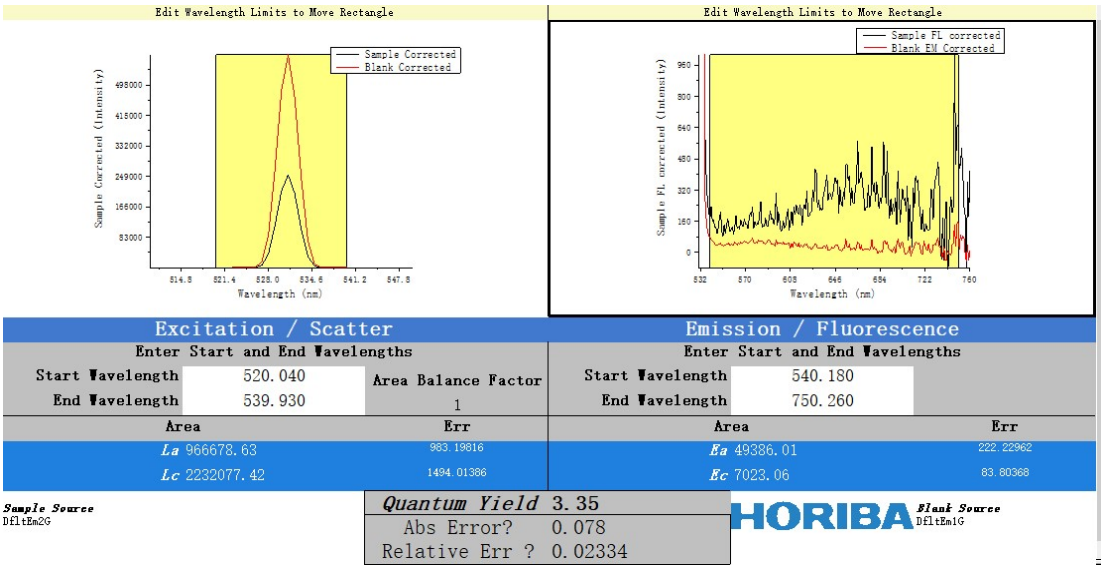

Figure S11. Quantum yield of **6DBF$_2$** in water.

Table S1. Optical properties of **6DBF$_2$** in different solvents.

solvent	λ_{abs} (nm)	ε ($M^{-1}\bullet cm^{-1}$)	λ_{em} (nm)	*Φ (quantum yield)*	*τ(fluorescence lifetime, ns)*
toluene	547	81600	599	55.89 %	2.963
Dimethyl sulfoxide	541	76290	595	1.93 %	0.104
water	548	48010	620	3.35 %	ND

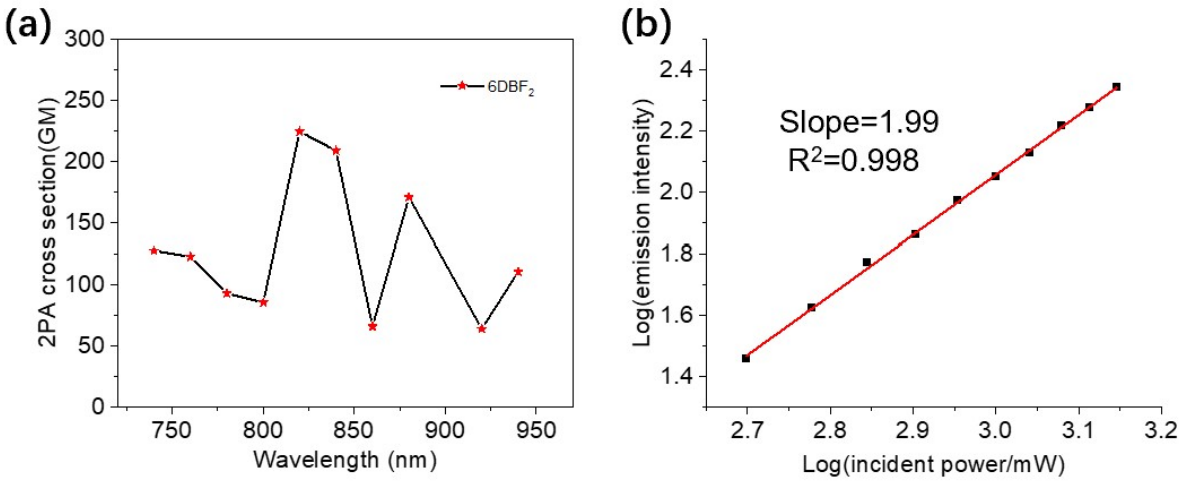

Figure S12. (a) Two-photon absorption cross-section (2PACS) spectra of **6DBF$_2$** in aqueous solution. (b) The dependence of two-photon excited fluorescence intensity of **6DBF$_2$** on excitation power intensity the femtosecond laser at 820 nm.

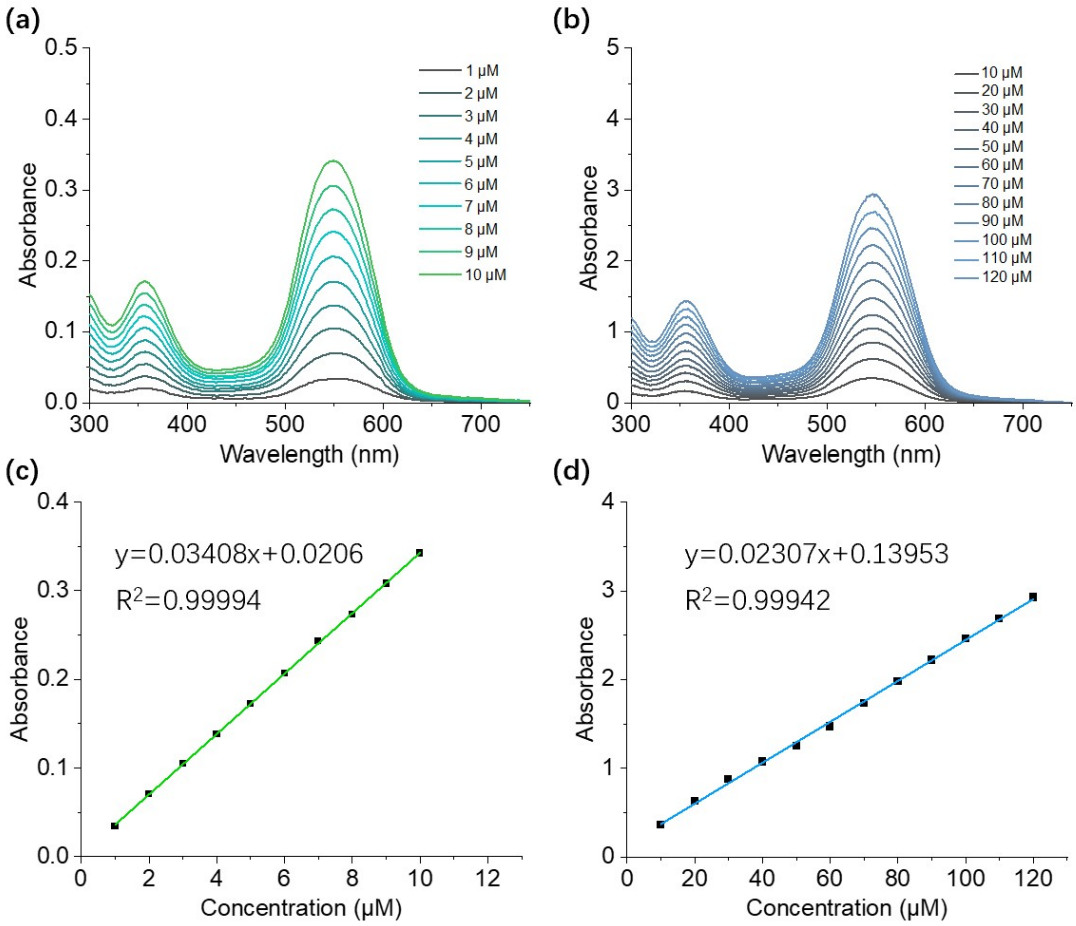

Figure **S13**. (a) (b) UV-Vis spectra of **6DBF$_2$** in H_2O in the presence of micro-dose DMSO. (c) (d)The relative plotting curves between absorbance versus concentration in H_2O.

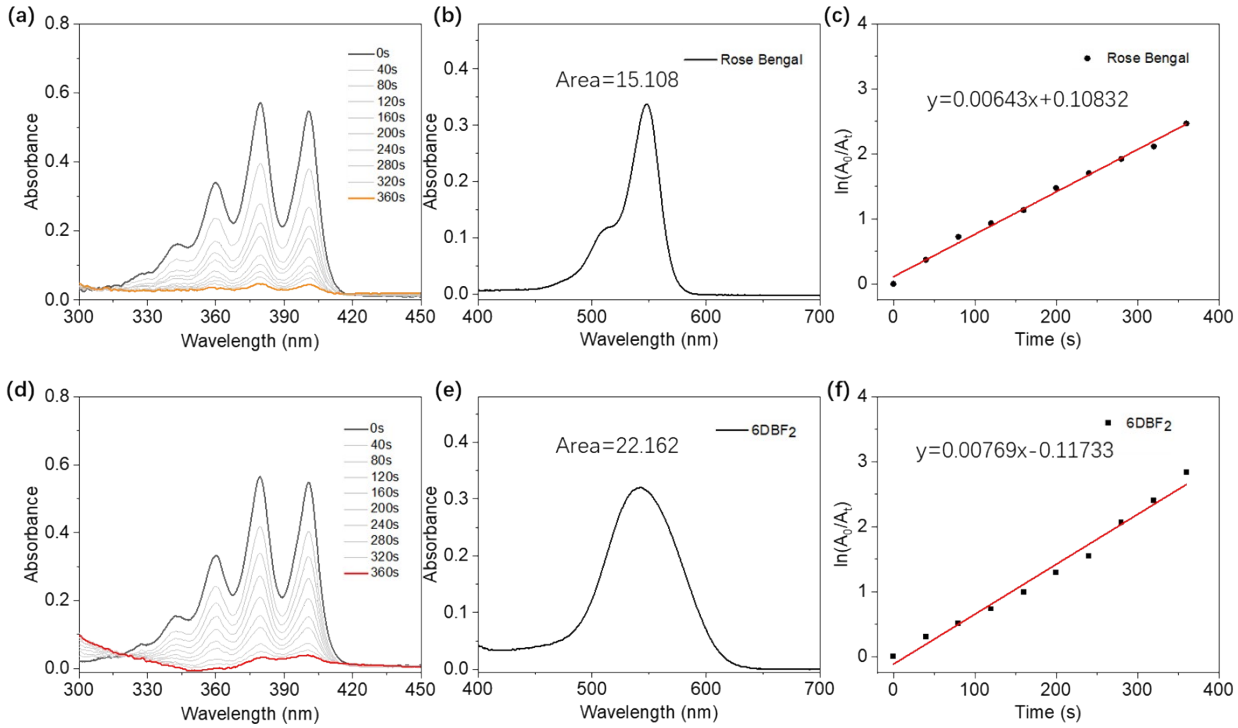

Figure S14. The UV-Vis spectra of ABDA (75 μM) in water under white light irradiation (0–360 s) in the presence of (a) Rose Bengal (10 μM) and (d) $6DBF_2$ (10 μM). The absorption spectrum of (b) rose Bengal and (e) $6DBF_2$ ranged in 400–700 nm. The absorbance decay of the ABDA at 378 nm under white light Irradiation (20 mW/cm^2) in the presence of (c) rose bengal and (f) **$6DBF_2$**.

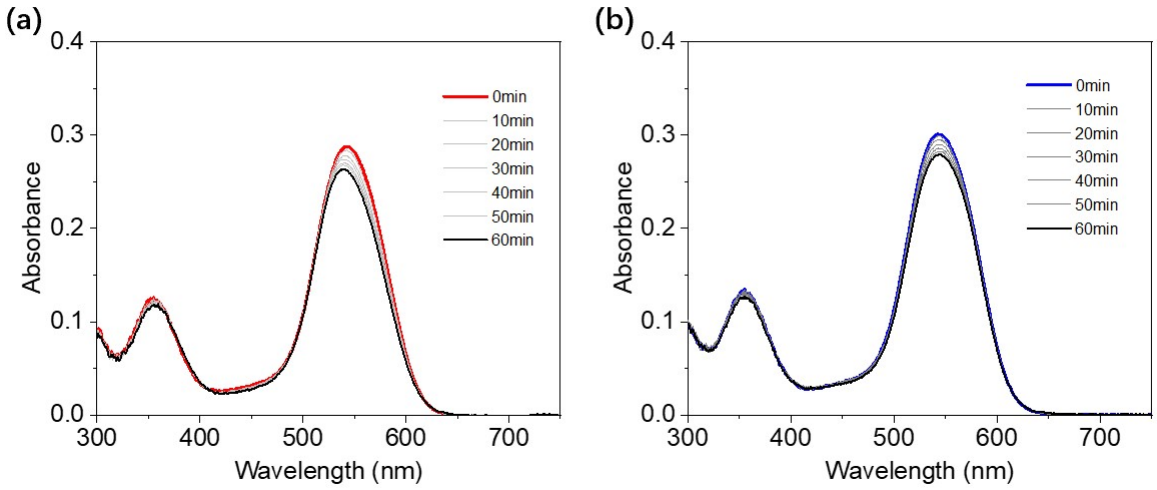

Figure S15. The UV-Vis spectra of **$6DBF_2$** in water when subject to (a) white light (20 mW/cm^2) or (b) 820 nm laser (100 mW) irradiation for 60 min.

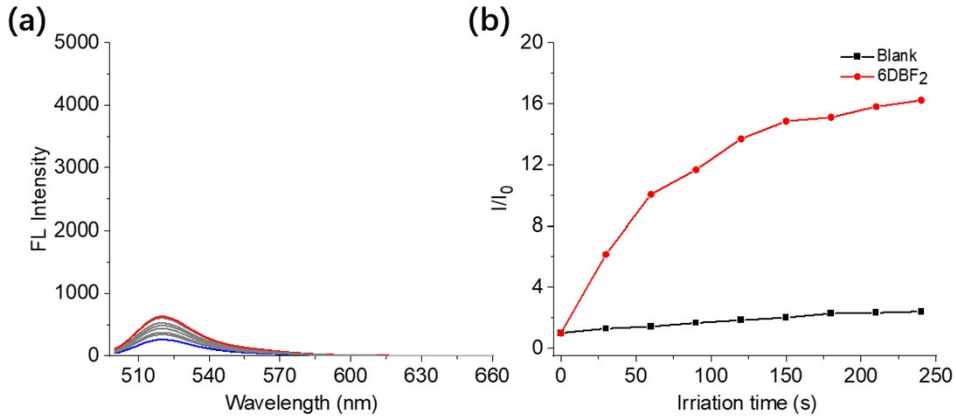

Figure S16. (a) Fluorescence spectra of DCFH-DA (40 μM, λex: 488 nm) in the inexistence of **6DBF$_2$** (10 μM) under different white light irradiation time (LED light, 400–700 nm, 20 mW/cm^2) in water. (b) Plotting curves of relative fluorescence intensity of DCFH-DA (I/I0, 10 μM, λex: 488 nm) versus the irradiation time in the absence and presence of **6DBF$_2$** in aqueous media under white light irradiation (LED light, 400–700 nm, 20 mW/cm2), where I_0 and I stands for the initial fluorescence intensity of DCFH-DA before and after irradiation.

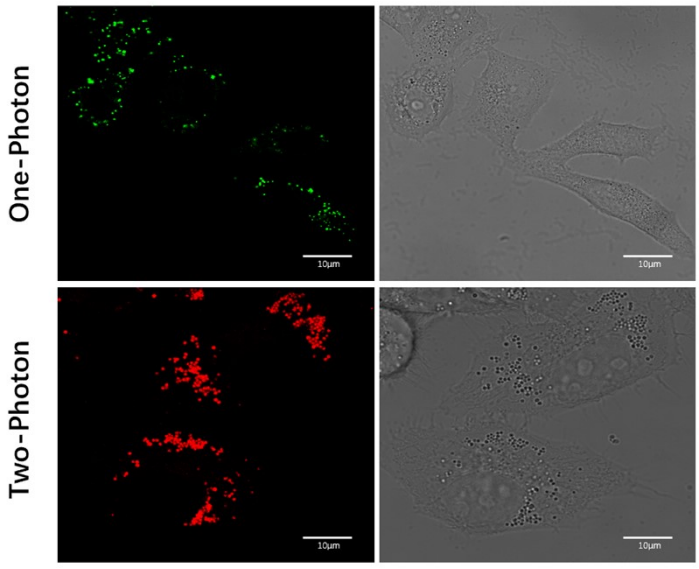

Figure S17. (a) One-photon and (b) two-photon confocal fluorescence images of HepG2 cells incubated with **6DBF$_2$** (0.5 μM) for 10 min. (a) λ_{ex}: 520 nm. λ_{em}: 590–630 nm. (b) λ_{ex}: 820 nm. λ_{em}: 590–630 nm. Scale bar = 10 μm.

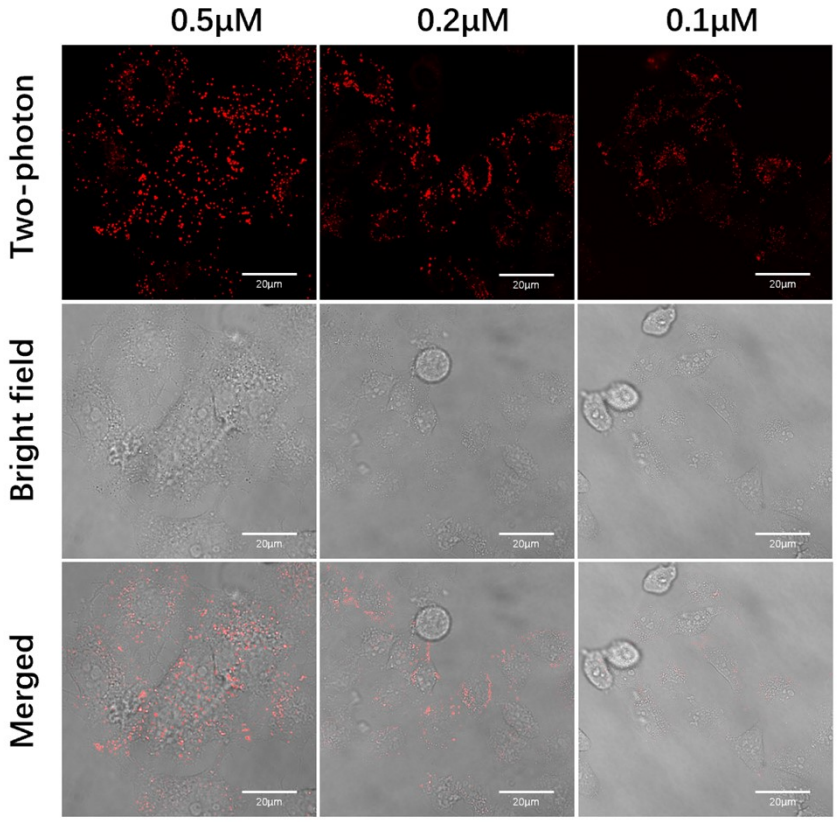

Figure 18. Bright-field and confocal images of living HepG2 cells after incubation with different concentrations of 0.5 μM, 0.2 μM and 0.1μM of **6DBF$_2$** for 30 min. λ_{ex}: 820 nm. λ_{em}: 590–630. Scale bar = 20 μm.

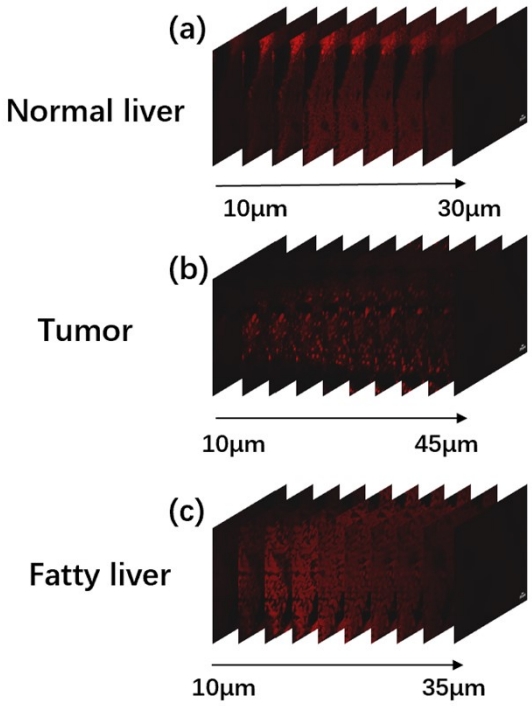

Figure S19. One-photon fluorescence images of normal hepatic tissues, HepG2 cancer tissues and fatty liver

tissues of mice treated with **6DBF$_2$** (1 mM) at different penetration depths. Scale bars: 20 μm.

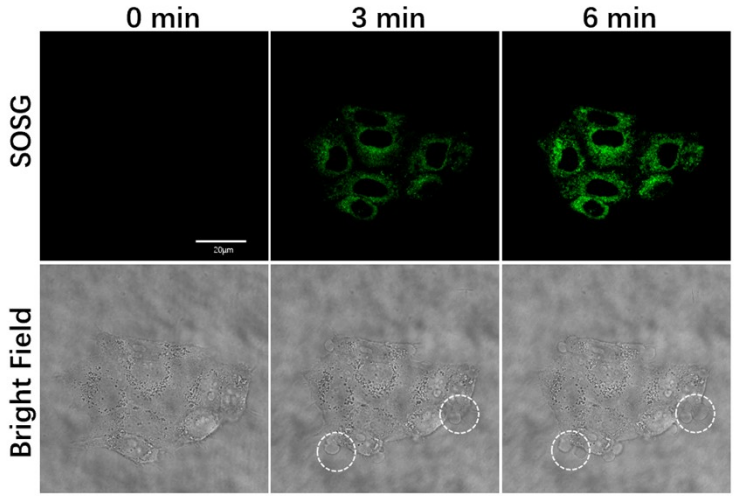

Figure S20. Confocal fluorescence images of HepG2 cells incubated with **6DBF$_2$** (1 μM) and SOSG (1 μM, λ_{ex}: 488 nm, λ_{em}: 500-530 nm) under white light irradiation. Scale bars: 20 μm.

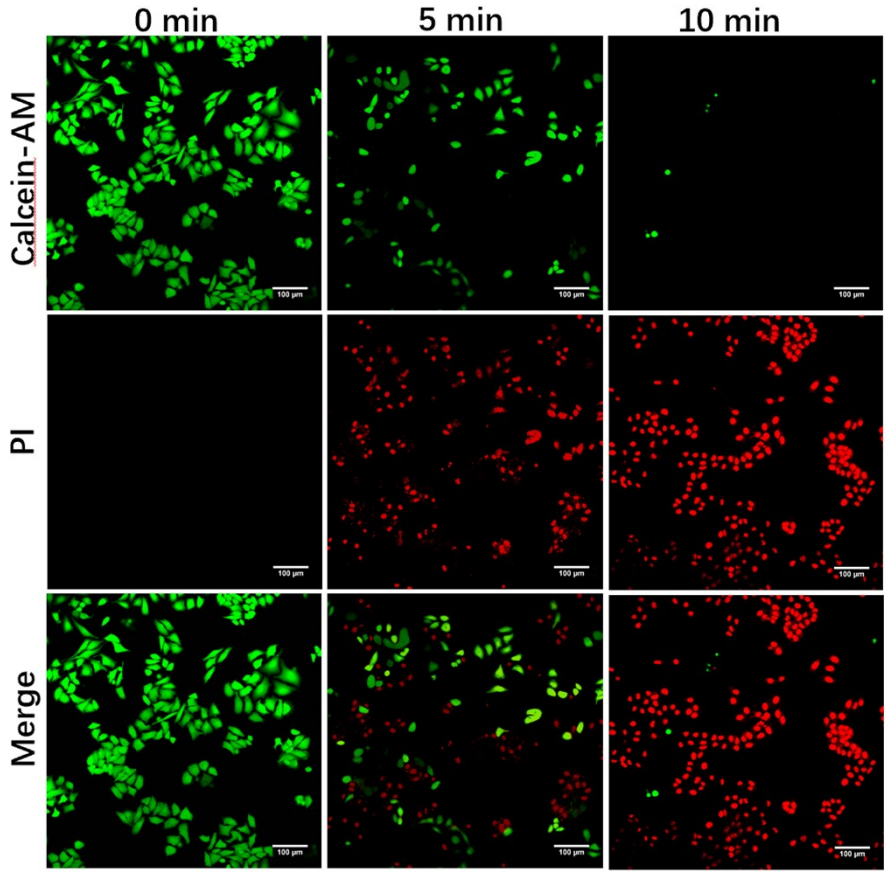

Figure S21. Confocal fluorescence images of HepG2 cells incubated with **6DBF$_2$** (5 μM) and co-stained with Calcein-AM(λ_{ex}: 488 nm, λ_{em}: 510 - 540 nm) and PI (λ_{ex}: 561 nm, λ_{em}: 590 - 620 nm) under dark or white light irradiation. Scale bars: 100 μm.

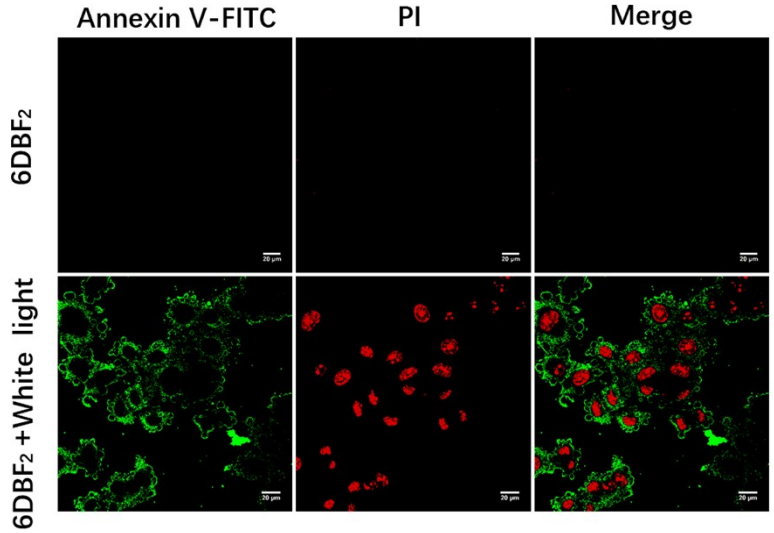

Figure S22. Confocal fluorescence images of Annexin V-FITC/PI and **6DBF$_2$** (5 μM) stained HepG2 cells under dark condition, white light irradiation. (green channel: λ_{ex}: 488 nm and λ_{em}: 500−540 nm; red channel: λ_{ex}: 561 nm and λ_{em}:630−670 nm). Scale bars: 20 μm.

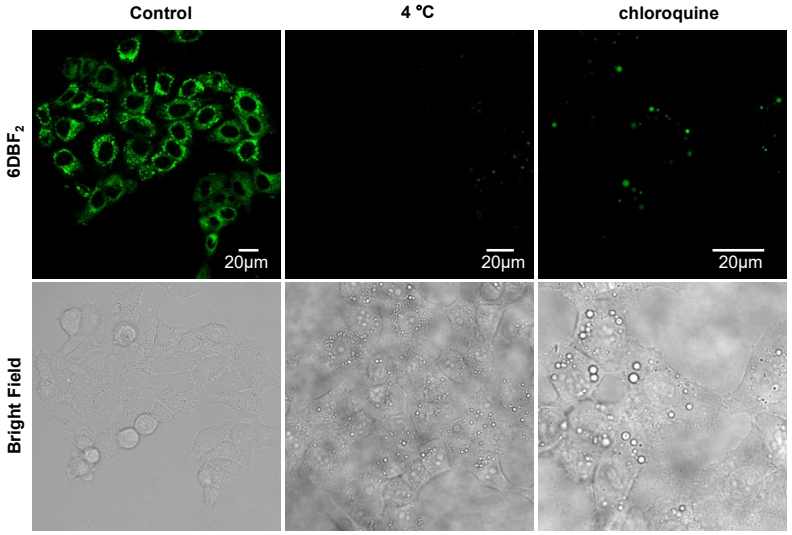

Figure S23. Confocal imaging of HepG2 cells treated with 6DBF$_2$(0.5 μM) at temperature of 4°C/37°C and in the absence/presence of chloroquine. Scale bar = 20 μm.

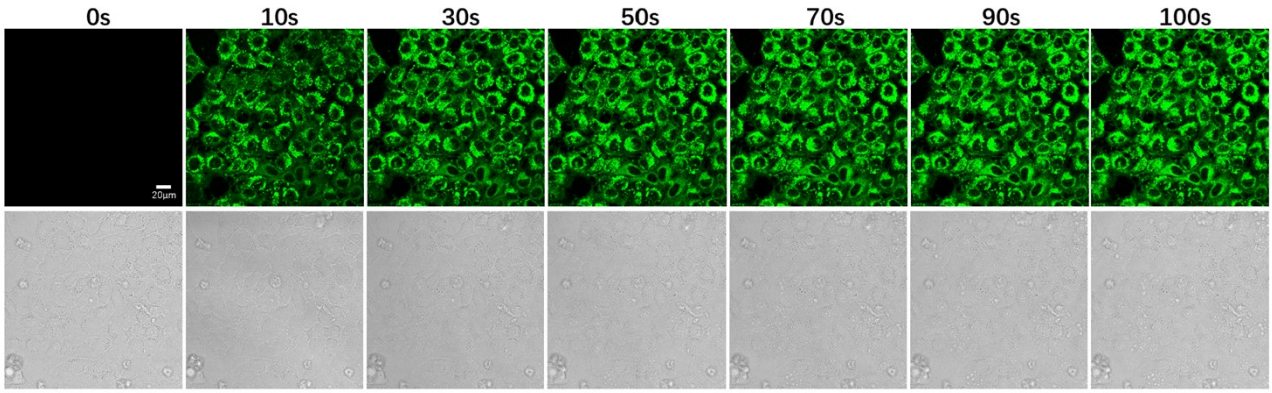

Figure S24. Confocal imaging of HepG2 cells treated with 6DBF$_2$ (0.5 μM) at different times. Scale bar = 20 μm.

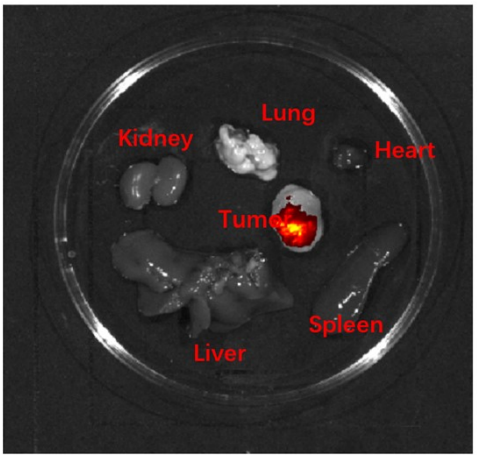

Figure S25. Fluorescence imaging of main organs (heart, liver, spleen, lung, kidney) in mice.

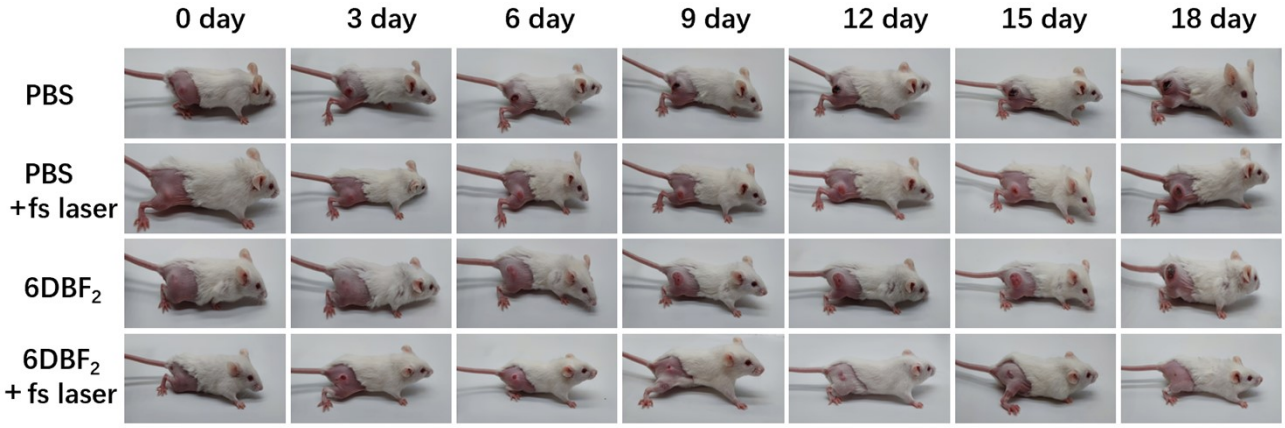

Figure S26. Photographs of H22 tumor-bearing mice of different groups taken during 18 days period after treatments.

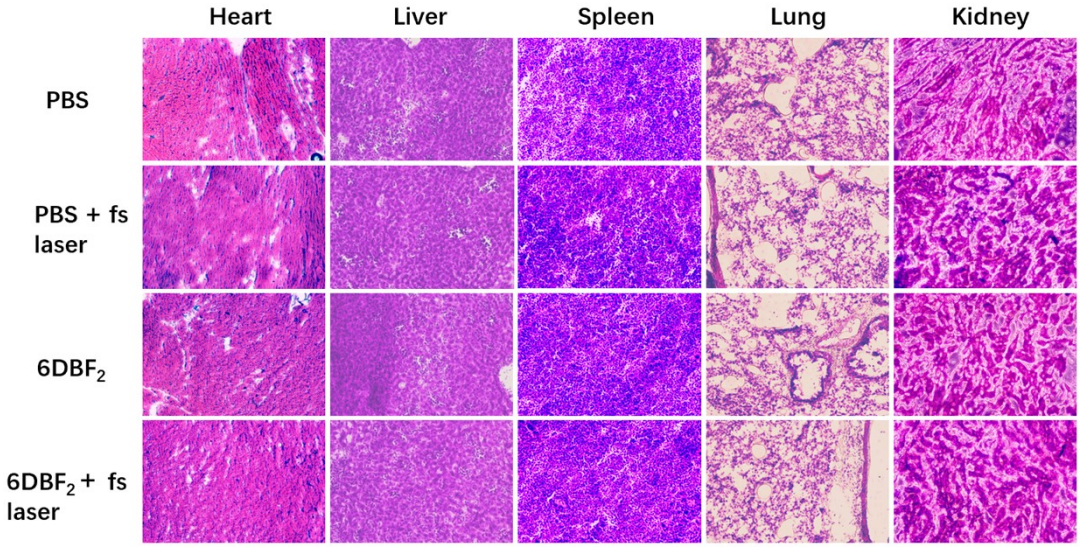

Figure S27. H&E-stained tissues of major organs dissected from different treatment groups.

4. Crystallographic Data

Table S2. Crystal data and structure refinement for **6DBF$_2$**.

Empirical formula	C31H27BF2N2S2
Formula weight	540.47
Temperature/K	296.15
Crystal system	orthorhombic
Space group	Pbcn
a/Å	28.180(7)
b/Å	9.279(2)
c/Å	23.837(6)
α/°	90
β/°	90
γ/°	90
Volume/Å3	6233(3)
Z	8
ρcalcg/cm3	1.152
μ/mm-1	0.204
Crystal size/mm3	0.25 × 0.12 × 0.11
Radiation	MoKα (λ = 0.71073)
2Θ range for data collection/°	2.89 to 55.09
Index ranges	-35 ≤ h ≤ 36, -11 ≤ k ≤ 11, -29 ≤ l ≤ 30
Reflections collected	47839
Independent reflections	6923 [Rint = 0.0968, Rsigma = 0.0748]
Data/restraints/parameters	6923/69/366
Goodness-of-fit on F2	1.020
Final R indexes [I>=2σ (I)]	R1 = 0.0706, wR2 = 0.1956
Final R indexes [all data]	R1 = 0.1653, wR2 = 0.2430
Largest diff. peak/hole / e Å-3	0.39/-0.51

Table S3. Bond Lengths for **6DBF$_2$**.

S1-C18	1.766(5)	C12-C13	1.454(6)
S1-C19	1.792(6)	C12-C18	1.374(6)
F1-B1	1.377(5)	C13-C14	1.392(6)
F2-B1	1.379(4)	C14-C15	1.523(7)
N1-C8	1.397(4)	C14-C16	1.388(7)
N1-C11	1.355(4)	C16-C17	1.366(7)
N1-B1	1.547(5)	C17-C18	1.414(6)
N2-C20	1.398(4)	C20-C21	1.406(4)
N2-C23	1.355(4)	C21-C22	1.373(5)
N2-B1	1.556(5)	C22-C23	1.398(5)
C1-C2	1.379(6)	C23-C24	1.498(4)
C1-C6	1.357(6)	C24-C25	1.383(5)
C2-C3	1.390(5)	C24-C30	1.394(5)
C3-C4	1.386(5)	C25-C26	1.408(5)

C4-C5	1.390(5)	C26-C27	1.505(5)
C4-C7	1.482(4)	C26-C28	1.368(5)
C5-C6	1.374(6)	C28-C29	1.363(5)
C7-C8	1.380(4)	C29-C30	1.391(5)
C7-C20	1.396(4)	C30-S2B	1.781(4)
C8-C9	1.411(4)	C30-S2A	1.804(12)
C9-C10	1.381(5)	S2B-C31B	1.734(6)
C10-C11	1.389(4)	S2A-C31A	1.763(19)
C11-C12	1.493(5)		

Table S4. Bond Angles for 1_a.

C18-S1-C19	102.8(3)	C16-C17-C18	120.4(5)
C8-N1-B1	125.0(3)	C12-C18-S1	119.2(3)
C11-N1-C8	107.6(3)	C12-C18-C17	117.9(5)
C11-N1-B1	127.1(3)	C17-C18-S1	122.7(4)
C20-N2-B1	124.1(3)	N2-C20-C21	108.5(3)
C23-N2-C20	107.0(3)	C7-C20-N2	121.6(3)
C23-N2-B1	128.8(3)	C7-C20-C21	129.5(3)
C6-C1-C2	120.1(4)	C22-C21-C20	107.0(3)
C1-C2-C3	120.0(4)	C21-C22-C23	107.9(3)
C4-C3-C2	120.0(4)	N2-C23-C22	109.7(3)
C3-C4-C5	118.7(3)	N2-C23-C24	124.6(3)
C3-C4-C7	120.5(3)	C22-C23-C24	125.7(3)
C5-C4-C7	120.7(3)	C25-C24-C23	120.1(3)
C6-C5-C4	120.6(4)	C25-C24-C30	119.9(3)
C1-C6-C5	120.6(4)	C30-C24-C23	119.8(3)
C8-C7-C4	121.0(3)	C24-C25-C26	121.6(3)
C8-C7-C20	120.7(3)	C25-C26-C27	120.8(4)
C20-C7-C4	118.3(3)	C28-C26-C25	117.1(3)
N1-C8-C9	107.4(3)	C28-C26-C27	122.1(3)
C7-C8-N1	121.3(3)	C29-C28-C26	122.1(3)
C7-C8-C9	131.3(3)	C28-C29-C30	121.4(4)
C10-C9-C8	107.8(3)	C24-C30-S2B	117.6(3)
C9-C10-C11	107.1(3)	C24-C30-S2A	125.6(5)
N1-C11-C10	110.1(3)	C29-C30-C24	117.9(3)
N1-C11-C12	122.7(3)	C29-C30-S2B	124.5(3)
C10-C11-C12	127.2(3)	C29-C30-S2A	111.6(8)
C13-C12-C11	117.8(4)	F1-B1-F2	110.6(3)
C18-C12-C11	119.7(4)	F1-B1-N1	110.7(3)
C18-C12-C13	122.3(4)	F1-B1-N2	109.0(3)
C14-C13-C12	117.0(5)	F2-B1-N1	108.7(3)
C13-C14-C15	116.8(6)	F2-B1-N2	110.6(3)
C16-C14-C13	120.0(5)	N1-B1-N2	107.3(3)

C16-C14-C15	123.2(5)	C31B-S2B-C30	105.2(2)
C17-C16-C14	122.2(5)	C31A-S2A-C30	97(2)

5. References

[1] V. C. G. David J. Jones, *Heterocycles* **2006**, *68*, 1121-1138.

[2] K. Nakano, K. Kobayashi, K. Nozaki, *J. Am. Chem. Soc.* **2011**, *133*, 10720-10723.

[3] L. Copey, L. Jean-Gérard, E. Framery, G. Pilet, B. Andrioletti, *Eur. J. Org. Chem.* **2014**, *2014*, 4759-4766.

[4] S. Dartar, M. Ucuncu, E. Karakus, Y. Hou, J. Zhao, M. Emrullahoglu, *Chem. Commun.* **2021**, *57*, 6039-6042.

[5] J. Tao, D. Sun, L. Sun, Z. Li, B. Fu, J. Liu, L. Zhang, S. Wang, Y. Fang, H. Xu, *Dyes Pigm.* **2019**, *168*, 166-174.